Icariin improves osteoporosis, inhibits the expression of PPARγ, C/EBPα, FABP4 mRNA, N1ICD and jagged1 proteins, and increases Notch2 mRNA in ovariectomized rats

HENGRUI LIU[1*], YINGQUAN XIONG[1*], XIAOFENG ZHU[2], HAN GAO[1], SUJUAN YIN[1], JIEFANG WANG[1], GUANGMING CHEN[1], CHAOPENG WANG[1], LU XIANG[1], PANPAN WANG[2], JI FANG[1], RONGHUA ZHANG[1] and LI YANG[1]

[1]Department of Traditional Chinese Pharmacology, College of Pharmacy, Jinan University; [2]Department of Traditional Chinese Medicine, First Affiliated Hospital, Jinan University, Guangzhou, Guangdong 510632, P.R. China

Received July 9, 2015; Accepted September 6, 2016

DOI: 10.3892/etm.2017.4128

Abstract. Icariin (ICA) is a pharmacologically active flavonoid glycoside that shows promise in the treatment and prevention of osteoporosis (OP). However, the mechanisms underlying the anti-osteoporotic effects of ICA remain largely unclear. The present study used quantitative polymerase chain reaction, western blot and immunohistochemical analysis to examine the effects of ICA on several key targets in the Notch signaling pathway in bone tissue in ovariectomized rats. It was observed that ICA has a pronounced beneficial effect on OP rats and inhibits the expression of peroxisome proliferator-activated receptor γ (PPARγ), CCAAT/enhancer binding protein α (C/EBPα) and fatty acid-binding protein 4 (FABP4) mRNA. In addition, it was identified that ICA downregulates the expression of notch1 intracellular domain (N1ICD) and Jagged1 proteins in bone tissue, and suppresses the effect of N1ICD on Notch2 mRNA expression. It is proposed that ICA inhibits the differentiation of mesenchymal stem cells into adipocytes by inhibiting the expression of PPARγ, C/EBPα and FABP4 mRNA via the Notch signaling pathway. In addition, it is proposed that ICA inhibits the expression of Notch2 mRNA by suppressing the effect of N1ICD. In conclusion, the results provide further mechanistic evidence for the clinical efficacy of ICA in the treatment of OP.

Correspondence to: Professor Ronghua Zhang or Dr Li Yang, Department of Traditional Chinese Pharmacology, College of Pharmacy, Jinan University, 601 Huangpu Avenue West, Guangzhou, Guangdong 510632, P.R. China
E-mail: tzrh@jnu.edu.cn
E-mail: doctormonkey@126.com

[*]Contributed equally

Key words: icariin, osteoporosis, Notch

Introduction

Osteoporosis (OP) is a metabolic bone disease that results from an imbalance between bone resorption and bone formation. OP is associated with decreased bone mass and damage to bone tissue microstructure that leads to an increased risk of fractures (1). As the world population ages, osteoporosis is becoming a global health problem.

Several drugs with a demonstrated anti-fracturative effects, achieved by inhibiting bone resorption or stimulating bone formation, are currently available for the treatment of OP (2). Their use, however, is not free from limitations or side effects. Compounds extracted from traditional Chinese medicines have been found to be safe and effective for the treatment of OP (3).

Icariin (ICA), a pharmacologically active prenylated flavonoid glycoside (Fig. 1), is one of the most abundant constituent in *Herba Epimedii*, a medicinal plant that has been used to treat OP in traditional Chinese medicine for thousands of years and is still currently used (4). Recent studies have shown that ICA exerts a variety of pharmacological activities, including antioxidant activity (5), immunoregulatory activity (6), antitumor activity (7,8) and estrogen-like activities (9,10). The promotion of osteogenesis (11) by ICA may be associated with its estrogen-like structure (12,13); in addition, ICA suppresses bone resorption and osteoclastogenesis (14-16).

Osseous tissue originates from mesenchymal stem cells (MSCs), which can differentiate into adipocytes or osteoblasts (OB) (17). The Notch signaling pathway is an important regulatory pathway that serves a key role in bone metabolism. The Notch signaling pathway mediates signaling between bone cells and is involved in the proliferation differentiation processes of bone cells (18). Notch proteins directly enhance osteogenic differentiation (19,20) and indirectly suppress osteogenic differentiation by promoting adipogenic differentiation (21,22), resulting in a two-directional regulatory effect on the differentiation of MSCs (21,22). To date, however, little effort has been made to understand the effect of ICA on the Notch signaling pathway. In the present study, the effect of ICA on proteins in the Notch signaling pathway, and its effect

on target genes, is investigated in an ovariectomized (OVX) rat model of OP.

Materials and methods

Animals. Specific pathogen-free (SPF) female Sprague-Dawley rats (aged 3 months and weighing 250±20 g) were provided by Guangdong Medical Laboratory Animal Center (Guangzhou, China). The study was approved by the Laboratory Animal Ethics Committee of Jinan University (ethical approval certificate no. SCXK 2013-0002).

Experimental medication. ICA (molecular weight, 676 g/mol; cat. no. EPE-120215) was provided by the Changsha Green Vine Biological Technology Co., Ltd. (Changsha, China). A reference sample (20 mg) of ICA (cat. no. 110737-200415) was purchased from the Guangdong Institute for Drug Control (Guangzhou, China). The ICA samples, which are insoluble in water, were stored in brown bottles. The ICA provided by the Changsha Green Vine Biological Technology Co., Ltd. was 98% pure, as compared with the reference sample. The positive control drug, Fosamax (cat. no. 130124), was purchased from MSD Pharmaceutical Co., Ltd. (Hangzhou, China).

Reagents. An alkaline phosphatase assay kit (cat. no. A059-2) was purchased from Nanjing Jiancheng Bioengineering Institute (Nanjing, China). Notch1 intracellular domain (N1ICD) and Jagged1 polyclonal antibodies were purchased from Abcam (Cambridge, MA, USA). Rabbit anti-rat GAPDH polyclonal antibody was purchased from Cell Signaling Technology, Inc. (Danvers, MA, USA; cat. no. 2118). Jagged2 polyclonal antibody was purchased from Merck Millipore (Darmstadt, Germany; cat. no. NRG1764426). Bovine serum albumin was purchased from Roche Diagnostics (Basel, Switzerland). PrimeScript RT Reagent kit with gDNE Eraser (cat. no. AK3501) and RT-PCR SYBR® (cat. no. AK4401) kits were purchased from TaKaRa Biotechnology Co., Ltd. (Dalian, China). Phenylmethanesulfonyl fluoride was purchased from Sigma-Aldrich (Merck Millipore). A bicinchoninic acid (BCA) protein assay kit was purchased from KeyGen Biotech. Co., Ltd. (Nanjing, China). An SDS-PAGE gel preparation kit, SDS-PAGE protein loading buffer (5X) and SDS-PAGE electrophoresis liquid were purchased from the Beyotime Institute of Biotechnology (Haimen, China). Goat anti-rabbit secondary antibody was purchased from EarthOx (Wuhan, China). Other commercially available reagents and chemicals used in the study were of analytical grade.

Instrumentation. The following equipment was used in the study: A dual X-ray absorptiometer (DEXA; Lunar iDXA; GE Healthcare Bio-Sciences, Pittsburgh, PA, USA), a microplate absorbance reader (model 680; Bio-Rad Laboratories, Inc., Hercules, CA, USA), a micro CT system (u-CT80; SCANCO Medical AG, Brüttisellen, Switzerland), a multi-function biomechanics tester (MTS model 858; Bionix, Toledo, OH, USA), an inverted phase contrast microscope (model CKX41; Olympus Corporation, Tokyo, Japan), a fluorescence spectrophotometer (NanoDrop 1000; Thermo Fisher Scientific, Inc., Waltham, MA, USA), a G-Storm Gradient PCR thermal cycler (Veriti 96-Well; Applied Biosystems; Thermo Fisher Scientific, Inc.), a quantitative fluorescence PCR system (Light Cycler® 480; Roche Diagnostics) and a gel imaging system (Bio-Rad Laboratories, Inc.).

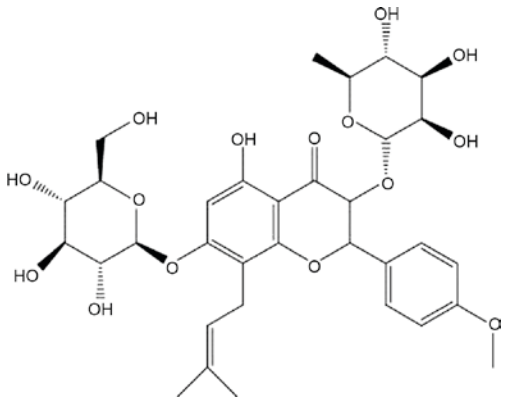

Figure 1. Chemical structure of icariin, a prenylated flavonoid glycoside.

Animal husbandry. SPF rats were reared by the Jinan University Medical Laboratory Animal Center and had *ad libitum* access to water and standard laboratory chow (1.01% Ca^{2+}, 0.78% P^{3+}).

Experimental design. Eighty-four rats were randomly divided into an ovariectomized (OVX) group (n=70) that would develop OP and a sham-operated group (n=14). After 12 weeks, rats underwent a dual-energy X-ray bone mineral density (BMD) test. Once the OP model was successfully established as previously described (23,24), the OVX group was randomly divided into the following five groups of 14 rats: A no treatment group (OVX-NT), a low-dose ICA group (ICA-L), a medium-dose ICA group (ICA-M), a high-dose ICA group (ICA-H) and a Fosamax-treated positive control group (FOS). The rats underwent treatment for 12 weeks.

ICA was dissolved in sodium carboxymethyl cellulose and administered by oral gavage. Fosamax was dissolved in distilled water and administered by oral gavage. The treatment regimens were as follows (Table I): i) Sham-operated, administered water (Sham group); ii) OVX, administered water (OVX-NT group); iii) OVX, administered 125 mg/kg/day ICA (ICA-L group); iv) OVX, administered 250 mg/kg/day ICA (ICA-M group); v) OVX, administered 500 mg/kg/day ICA (ICA-H group); and vi) OVX, administered 0.514 mg/kg/day Fosamax (FOS group).

Dual-energy x-ray absorptiometry (BMD). After 12 weeks, BMD was tested by dual X-ray scans. The rats were then anesthetized using pentobarbital sodium (0.15 ml/100 g; Vortech Pharmaceuticals, Ltd., Dearborn, MI, USA) and whole body scans were conducted. Bone mineral densities of the whole body, femora, tibias, and fourth and fifth lumbar vertebrae (LV4, 5) were measured following sacrifice using an overdose of pentobarbital sodium (0.4 ml/100 g).

Micro-CT. Tibia, femora and LV4, 5 were separated, dissected free of soft tissues and stored at -80˚C for subsequent analysis. The microarchitecture of trabecular bone in the right proximal femora and LV4 was analyzed by micro CT (60 KV, 50 W). The same specimen was scanned to obtain different section images

Table I. Treatment groups.

Group	Model	Drug	Dose (mg/kg/day)	Dosing period (weeks)	Administration
Sham	Sham	Water	-	12	Oral gavage
OVX-NT	OVX	Water	-	12	Oral gavage
ICA-L	OVX	ICA	125	12	Oral gavage
ICA-M	OVX	ICA	250	12	Oral gavage
ICA-H	OVX	ICA	500	12	Oral gavage
FOS	OVX	Fosamax	0.514	12	Oral gavage

OVX, ovariectomized; OVX-NT, OVX-no treatment group; ICA, icariin; ICA-L, low-dose ICA group; ICA-M, medium-dose ICA group; ICA-H, high-dose ICA group; FOS, Fosamax-treated positive control group.

and the distal femoral stem epiphyseal and vertebral scans were performed in three spatial dimensions. Micro View software (version 4.1; Scanco Medical AG, Wangen-Bruttisellen, Switzerland) was used to calculate the following parameters: Trabecular thickness, trabecular number and trabecular separation.

Immunohistochemical staining. One third of the right distal femur was fixed with 4% paraformaldehyde and decalcified using the Aojiang decalcification method as follows: The femur was fixed in 20% EDTA for decalcification at 4˚C, dehydrated and embedded in paraffin. Five micron paraffin sections were prepared for immunohistochemical staining. Slices were dewaxed using xylene and hydrated with gradient alcohol. Endogenous peroxidase activity was quenched (using 3% hydrogen peroxide) and the slices were then incubated with Jagged1 primary antibody (1:1,000) at 37˚C for 1 h. The slices were then washed three times with phosphate buffer, incubated with streptavidin-horseradish peroxidase (HRP)-conjugated anti-rabbit secondary antibody (1:2,000; cat. no. 7074S; Cell Signaling Technology, Inc.) at 37˚C for 10 min and washed another three times with phosphate buffer. Diaminobenzidine-colored slices were then stained with hematoxylin and dehydrated using alcohol. Xylene was added and the slices were sealed using neutral gum. A light microscope was used to view the stains.

Reverse transcription-quantitative polymerase chain reaction (RT-qPCR). Chopped rat femora were treated with liquid nitrogen and ground to a powder. Total RNA was extracted from the femora by triturating several times with TRIzol reagent (Thermo Fisher Scientific, Inc.) and allowed to stand at room temperature for 5 min. Chloroform (1/5 of the volume of Trizol) was added and the sample was blended in a vortex mixer. After standing at room temperature for 5 min, the mixture was centrifuged (12,000 x *g*) for 5 min at 4˚C. The top 70% of the aqueous phase (0.5 ml) was transferred to an Eppendorf tube and shaken with isopropyl alcohol (0.25 ml), 0.8 M aqueous sodium citrate solution (0.125 ml) and 0.125 M aqueous NaCl solution (0.8 ml). After standing at room temperature for 10 min, the mixture was centrifuged (12,000 x *g*) for 15 min at 4˚C. After washing twice with 75% ethanol, the sediment was dissolved in diethylpyrocarbonate (DEPC)-treated water (20 μl). Avoiding bubbles, RNA samples (1 μl) were placed in the spectrophotometer and the ratio (A260/A280) of absorbance at 260 nm (A260) and 280 nm (A280) was determined to provide an assessment of purity. Total RNA (1 μg) was reverse transcribed into cDNA. Template DNA was used in gene-specific PCR for PPARγ, C/EBPα, FABP4, Notch2 and GAPDH mRNA. Details of the primers are listed in Table II. qPCR for gene expression was performed in 96-well plates with a total reaction volume of 20 μl per well, comprising 2x SYBR green master mix, diluted gene primers (10 μl), cDNA (2 μl), forward primer (0.8 μl) or reverse primer (0.8 μl), and DEPC-treated water (6.4 μl). Quantitative analysis was performed using a Roche LightCycler 480 Sequence Detection System. Operating conditions were 95˚C for 30 sec, 95˚C for 5 sec and 60˚C for 30 sec, with a total of 40 cycles. The fluorescence signal was collected at the end of the second step of each cycle. Each sample was analyzed in triplicate and the average Cq was calculated. Gene expression was analyzed using the $2^{-\Delta\Delta Cq}$ quantification approach (25).

Table II. Primer sequences for quantitative fluorescence polymerase chain reaction.

Gene name	Primer sequence (5'-'3)
PPARγ-sense	ACCCTTTACCACGGTTGATTTCTC
PPARγ-antisense	CAGGCTCTACTTTGATCGCACTTT
C/EBPα-sense	GCGCAAGAGCCGAGATAAAG
C/EBPα-antisense	CGTGTCCAGTTCACGGCTCA
FABP4-sense	ACATGAAAGAAGTGGGAGTTGGC
FABP4-antisense	AAGTACTCTCTGACCGGATGACG
Notch2-sense	AGTGGTATGGACTGTGAGGAGG
Notch2-antisense	CAGGAGAAGGTGTTCACTTTGTC
GAPDH-sense	CAACGGGAAACCCATCACCA
GAPDH-antisense	ACGCCAGTAGACTCCACGACAT

PPARγ, peroxisome proliferator-activated receptor γ; C/EBPα, CCAAT/enhancer binding protein α; FABP4, fatty acid-binding protein 4.

Western blotting analysis. Rat femora were subjected to cell lysis to extract proteins. The concentration of total protein was determined using a BCA protein assay kit. Proteins

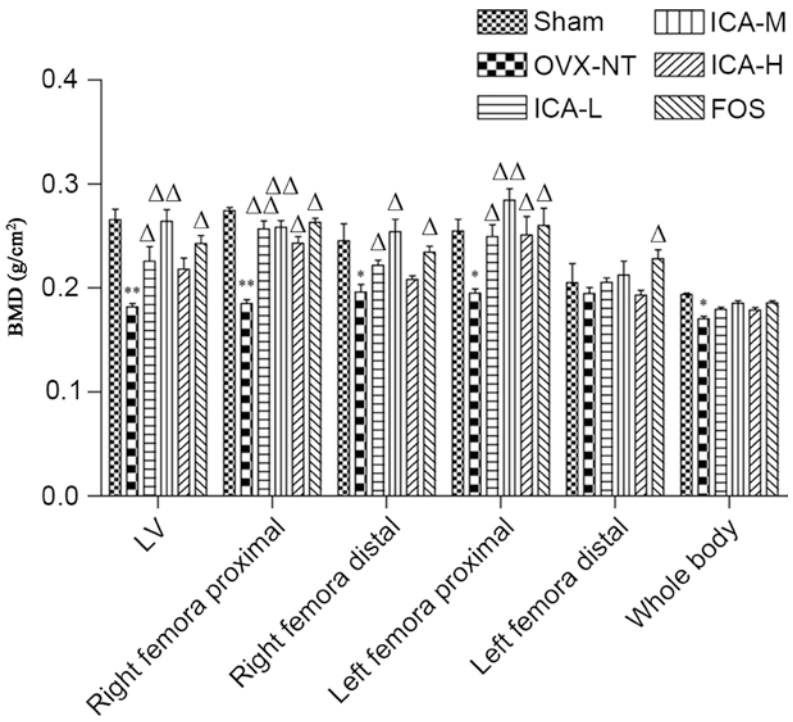

Figure 2. ICA treatment increases BMD. After 12 weeks of treatment, mice were anesthetized and whole body scans were conducted. BMD of the whole body, femora and tibias, as well as the fourth and fifth lumbar vertebrae, were measured. *P<0.05, **P<0.01 vs. the sham-operated group; $^{\Delta}$P<0.05, $^{\Delta\Delta}$P<0.01 vs. the OVX-NT group. BMD, bone mineral density; OVX-NT, ovariectomized-no treatment group; ICA-L, low-dose icariin group; ICA-M, medium-dose icariin group; ICA-H, high-dose icarrin group; FOS, Fosamax-treated positive control group; LV, lumbar vertebrae.

Table III. Comparisons with the sham-operated group.

Group	LV4, 5	Right femur	Left femur
Sham	0.285±0.009	0.340±0.020	0.310±0.013
OVX-NT	0.212±0.006[a]	0.262±0.006[a]	0.247± 0.005[a]

[a]P<0.05 vs. the sham-operated group. Data are presented as the mean ± standard deviation. LV4, 5, fourth and fifth lumbar vertebrae; OVX-NT, ovariectomized-no treatment group.

(30 μg) were separated by 12% SDS-PAGE and transferred onto polyvinylidene difluoride membranes. Membranes were blocked with a buffer containing 0.05% Tween-20 and 5% defatted milk and reacted sequentially with primary antibodies against GAPDH and N1ICD (1:1,000) for 10 h at 4˚C and HRP-conjugated anti-rabbit secondary antibody (1:3,000) for 1 h at 25˚C. The membranes were washed and rinsed with enhanced chemiluminescence (ECL) detection reagents (EMD Millipore, Billerica, MA, USA). The band images were photographed using ECL. Immunoreactive bands were visualized using ECL substrates and an X-ray film processor. Protein expression was calculated using Quantity One® software (version 6.0; Media Cybernetics, Inc., Rockville, MD, USA).

Statistical analysis. Values are expressed as the mean ± standard deviation. The significance of the difference between two experimental groups was estimated by one-way analysis of variance. P<0.05 was considered to indicate a statistically significant difference. All statistical evaluations were performed using SPSS version 19.0 (IBM SPSS, Amronk, NY, USA).

Results

Establishment of the OP model. Twelve weeks after OVX, BMD of the LV4, 5, right femur and left femur was significantly reduced in the OVX-NT group compared with the sham-operated group (P<0.05), demonstrating that the OP model had been established successfully (Table III).

ICA treatment increases BMD. BMD was measured using dual-energy X-ray absorptiometry. BMD was significantly lower (P<0.05) in the right distal femora, left primal femora and whole body bone regions in the OVX-NT group compared with the sham-operated group. In addition, BMD in the lumbar spine and right proximal femora were significantly reduced compared with the sham-operated group (P<0.01). BMD of the lumbar spine, the left proximal femora and right proximal femora in the FOS and ICA groups were significantly increased compared with the OVX-NT group (P<0.05 and P<0.01), except the ICA-H group in the lumbar spine. BMD in the ICA-M group showed the most significant difference compared with the OVX-NT group (P<0.01) (Fig. 2).

ICA treatment improves bone trabeculae. Micro CT showed that the bone trabecular number in the right distal femora and LV4 was higher, and that the bone trabecular separation degree was smaller, in the sham-operated group compared with the OVX-NT group. In the OVX-NT group, the bone trabeculae were rod-shaped, thinner and fractured, and the

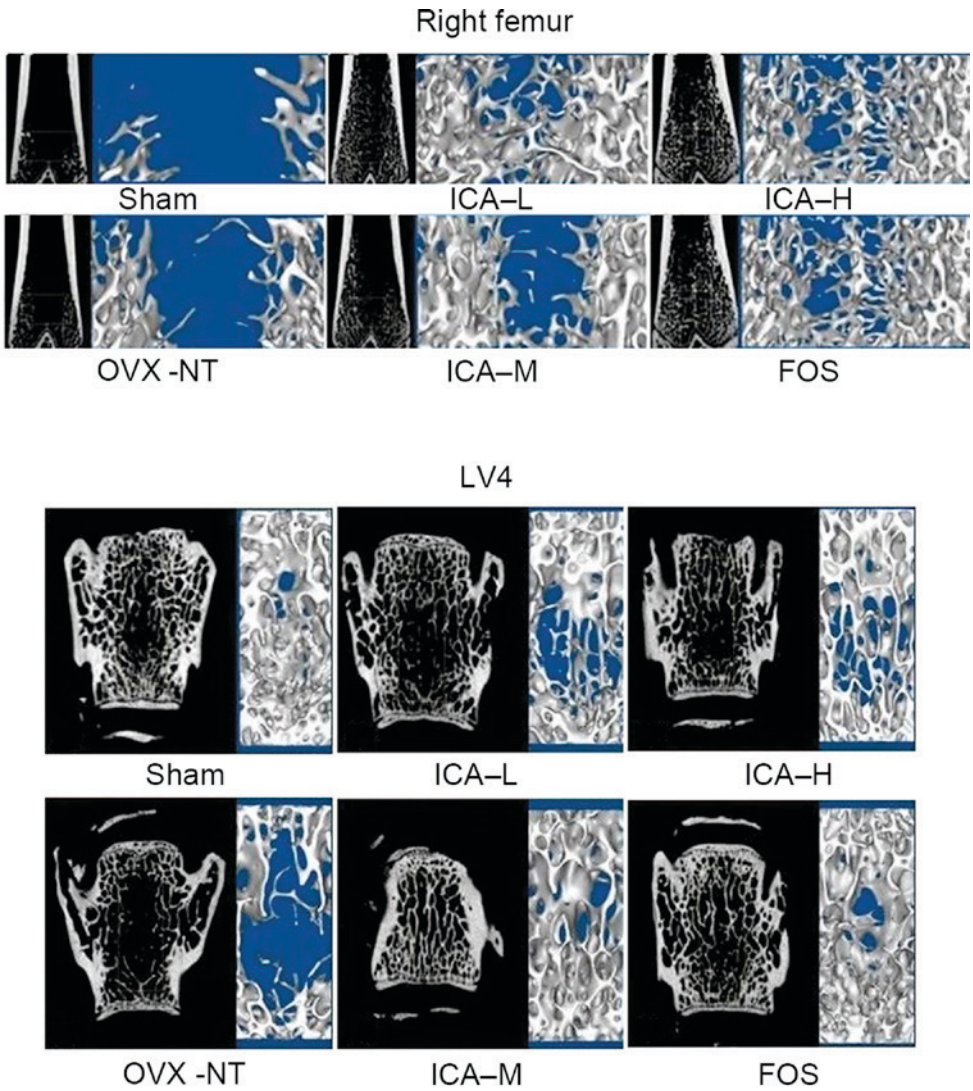

Figure 3. ICA treatment improves bone trabeculae. Microarchitecture of trabecular bone was analyzed using micro computed tomography. Bone trabecular number in the right distal femora and LV4 increased, and the degree of bone trabecular separation became smaller in the sham-operated group. Bone trabeculae were rod-shaped, thinner, and fractured and bone trabecular separation increased in the OVX-NT group. Compared with the OVX-NT group, bone trabecular number increased in the ICA-L, ICA-M, ICA-H and FOS groups, particularly in the ICA-M and FOS groups, where bone trabecular thickness tended towards that of the sham-operated group. Although bone trabecular separation was reduced, some trabecular bone was missing; bone trabecular separation increased in the ICA-L group, but there was some improvement compared with the OVX-NT group. OVX, ovariectomized group; OVX-NT, OVX-no treatment group; ICA-L, low-dose icariin group; ICA-M, medium-dose icariin group; ICA-H, high-dose icarrin group; FOS, Fosamax-treated positive control group; LV4, fourth lumar vertebra.

bone trabecular separation was increased. Compared with the OVX-NT group, bone trabecular number was higher in the treated groups, particularly in the ICA-M and FOS groups. In the treated groups, bone trabecular thickness tended towards that in the sham-operated group. Although bone trabecular separation was reduced, some trabecular bone was missing. Bone trabecular separation increased in ICA-L group, but there displayed some improvement compared with the OVX-NT group (Fig. 3).

ICA inhibits the expression of PPARγ, C/EBPα, and FABP4 mRNA and increases Notch2 mRNA. Compared with the sham-operated group, the expression of PPARγ, C/EBPα and FABP4 mRNA was significantly increased (P<0.05) and the expression of Notch2 mRNA was decreased in the OVX-NT group (P<0.05). Compared with the OVX-NT group, the expression of PPARγ, C/EBPα and FABP4 mRNA expression was significantly decreased (P<0.05) and Notch2 mRNA expression was significantly increased in the ICA-M group (P<0.05) (Fig. 4).

ICA inhibits the expression of N1ICD protein. Western blotting showed that, compared with the sham-operated group, expression of N1ICD was significantly increased (P<0.05) in the OVX-NT group. Compared with the OVX-NT group, expression of N1ICD decreased in the ICA-M group (P<0.01) (Fig. 5).

ICA inhibits the expression of Jagged1 protein. Immunohistochemistry showed that Jagged1 was distributed in the bone marrow cavity on fat cell membranes. Compared with the sham-operated group, the expression of Jagged1 protein increased in the OVX-NT group and, compared with the OVX-NT group, the expression of Jagged1 protein

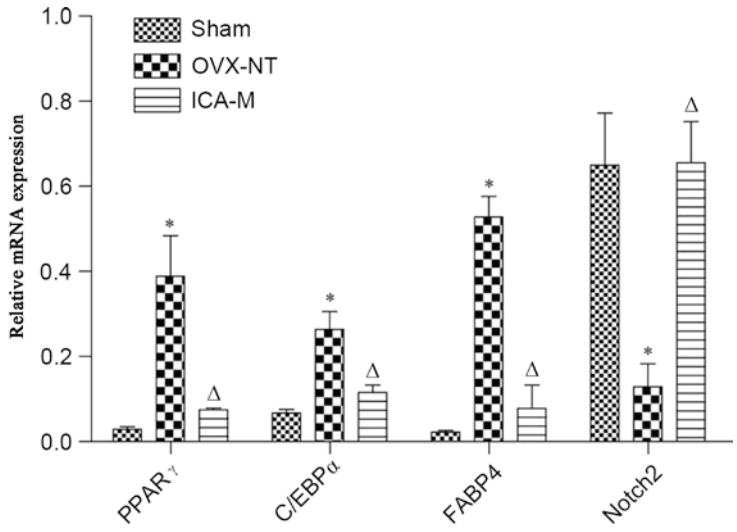

Figure 4. ICA inhibits the expression of PPARγ, C/EBPα and FABP4 mRNA and increases Notch2 mRNA. Total RNA was extracted from the femora and quantitative polymerase chain reaction for each gene expression was performed. *P<0.05 vs. the sham-operated group; ΔP<0.05 vs. the OVX-NT group. OVX-NT, ovariectomized-no treatment group; ICA-M, medium-dose icarrin group; PPARγ, peroxisome proliferator-activated receptor γ; C/EBPα, CCAAT/enhancer binding protein α; FABP4, fatty acid-binding protein 4.

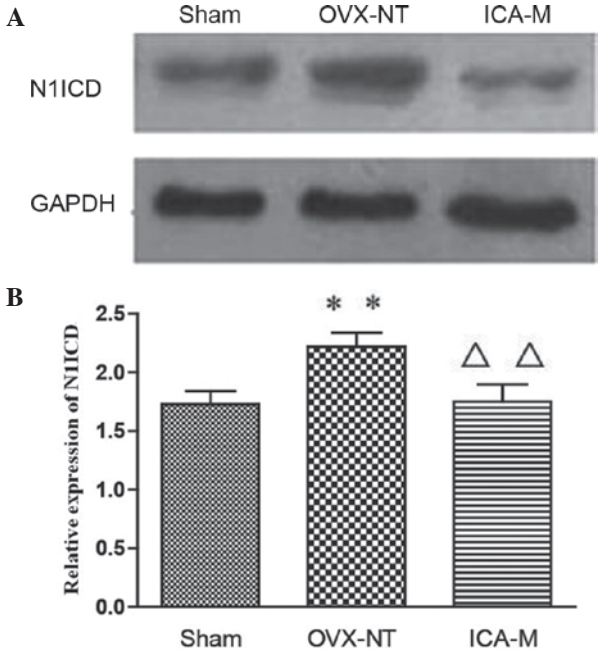

Figure 5. ICA inhibits the expression of N1ICD protein. Rat femora were subjected to cell lysis to extract proteins. Expression of GAPDH and N1ICD protein was detected by (A) western blot and (B) quantified. Compared with the sham-operated group, expression of N1ICD increased in the OVX-NT group. Compared with the OVX-NT group, expression of N1ICD decreased in the ICA-M group. **P<0.01 vs. the sham group; ΔΔP<0.01 vs. the OVX group. OVX-NT, ovariectomized-no treatment group; ICA-M, medium-dose icarrin group; N1ICD, Notch1 intracellular domain.

decreased in the ICA-M group (Fig. 6). The average density was determined using Image-Pro Plus version 6.0 image analysis software (Media Cybernetics, Inc.). Compared with the sham-operated group, the expression of Jagged1 protein increased significantly in the OVX-NT group (P<0.01) and, compared with the OVX-NT group, expression of Jagged1 protein decreased in the ICA-M group.

Discussion

Despite the lack of a clearly defined pharmacological mechanism of action, previous studies have demonstrated that ICA, extracted from the dried leaves of the medicinal plant *Herba Epimedii*, stimulates osteogenic differentiation *in vitro* and prevents bone loss in vivo (26-31). Because of its low toxicity and favorable side effect profile, ICA would be an attractive and promising candidate for the treatment and prevention of OP (30). The present study helps to explain the pharmacological mechanism of action of ICA in preventing bone loss in OVX rats.

Fosamax was chosen as the positive control since it is known to increase bone mineral density (31). The present study shows that ICA effectively reduces bone mass loss in OVX rats, increases bone trabecular number and thickness, reduces the degree of separation of trabecular bone, and improves its morphological structure. ICA-M showed the most pronounced effect on these indices, indicating that ICA-M has the greatest therapeutic effect in osteoporosis and, perhaps, suggesting a bell-shaped dose-response curve.

A reduced capacity of MSCs for osteogenesis and an increased capacity for adipogenesis, which results in an imbalance between bone resorption and bone formation, serves an important role in the pathogenesis of OP (32). These biological processes are partially regulated by the activation of the Notch signaling pathway, the primary focus of the present study.

The Notch receptor family consists of four receptors: Notch 1, 2, 3 and 4. Notch ligands are transmembrane proteins with conserved structures. In mammals, there are five known Notch ligands: Delta 1, 3 and 4 and Jagged1 and 2. Ligand binding to receptors results in successive proteolytic cleavage mediated by TADE metalloproteases and a γ-secretase complex. Cleavage of the Notch receptor results in the release of a constitutively active Notch intracellular domain (NICD) that translocates to the nucleus, where it binds with the transcription complex CSL/CBF1. NICD switches the CSL/CBF1 complex from a repressed to an activated state, which promotes cell

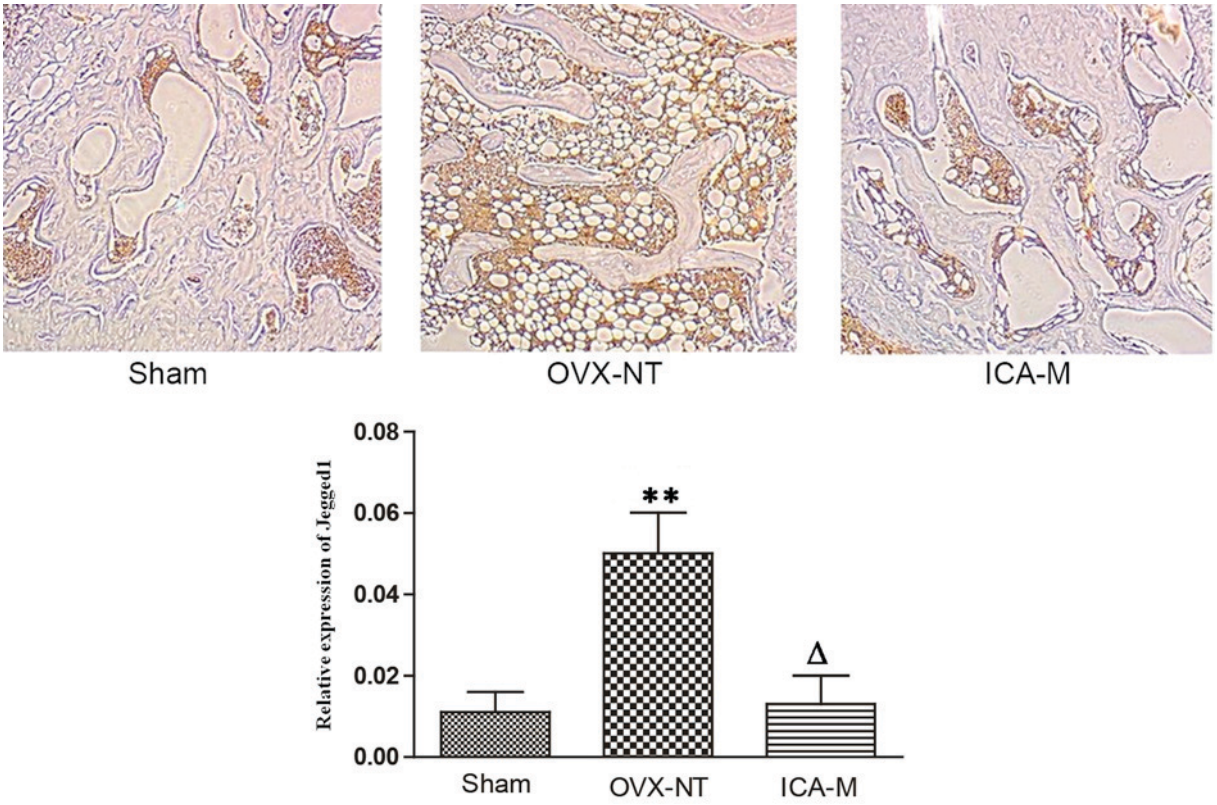

Figure 6. ICA inhibits the expression of jagged1 protein. (A) One third of the right distal femur was fixed with 4% paraformaldehyde and decalcified using the Aojiang decalcification method. Magnification, x40. (B) Compared with the sham-operated group, expression of Jagged1 protein increased in the OVX-NT group. Compared with the OVX-NT group, expression of Jagged1 protein decreased in the ICA-M group. **P<0.01 vs. the sham group; $^{\Delta}$P<0.01 vs. the OVX group. OVX-NT, ovariectomized-no treatment group; ICA-M, medium-dose icarrin group.

differentiation, proliferation and apoptosis. Campa *et al* (33) showed that the Notch1-Jagged1 pathway is active in MSCs during OB differentiation, indicating a regulatory role for Notch signaling in OB differentiation. Jagged1 is an essential ligand for activation of Notch in the early stages of chondrogenesis, but expression of Jagged1 is downregulated at later stages of the process (34). NICD is one of the nuclear signaling molecules that suppresses differentiation of OB. Transfection with Jagged1 and Delta1 genes enhances the activity of alkaline phosphatase and increases mineralization (19). This improves differentiation of mouse embryo MSCs through osteoblast induction, and suppresses the expression of lipogenic genes (such as FABP4 and PPARγ) in MSCs through promotion of adipogenesis (35). Bai *et al* (36) identified that knockout of Notch1, Notch2 and Notch3 in bone macrophagocytes increases the differentiation of mononuclear macrophages into OC, and that deficiency of Notch1 reduces the release of osteoprotegerin. Activation of Notch signaling thus enhances the differentiation of MSCs into adipocytes and suppresses their differentiation into OB (21,22).

The present study shows that ICA treatment suppresses the expression of N1ICD and Jagged1 proteins, and promotes the expression of Notch2 mRNA. N1ICD is the active intracellular form of the Notch1 receptor, which serves an important role within the cell by regulating downstream target genes (37,38). This suggests that the beneficial effect of ICA on OP may be associated with the regulation of Notch signaling, which increases the expression of adipocyte differentiation transcription factors. The results of the present study agree with those of Zanotti *et al* (39), which showed that an increase in N1ICD reduces the expression of Notch2 mRNA. It is proposed, therefore, that Notch2 depresses Notch signaling, through negative feedback of Notch1.

PPARγ and C/EBP family proteins are two of the primary transcription factors that directly affect preadipocyte proliferation and differentiation. Ugarte *et al* (40) identified that the enhancement of Notch signaling suppresses the differentiation of MSCs into adipocytes by inhibition of PPARγ and FABP4 gene expression. The inhibition of osteogenesis is possibly associated with PPARγ, one of the important factors controlling adipogenic differentiation. Once activated, PPARγ can spontaneously initiate the process of adipogenic differentiation (19). C/EBPα was the first transcription factor proven to serve an important role in the process of adipocyte differentiation (41). Additionally, there is a synergistic interaction between C/EBPα and PPARγ. PPARγ activates C/EBPα expression, and C/EBPα has a positive feedback effect on PPARγ. The combination of C/EBPα and PPARγ activates the expression of genes associated with differentiation. The expression of PPARγ mRNA and C/EBPα mRNA directly reflects the adipocyte differentiation status of MSCs.

In the present study, the expression of PPARγ, C/EBPα and FABP4 mRNA were significantly reduced following treatment with ICA (250 mg/kg/day). This is in agreement with a study by Lewis *et al* (42), which showed that PPARγ, C/EBPα and FABP4 mRNA are significantly increased in animals with OP compared with normal animals. The pathogenesis of OP was thus shown to be closely associated with enhanced

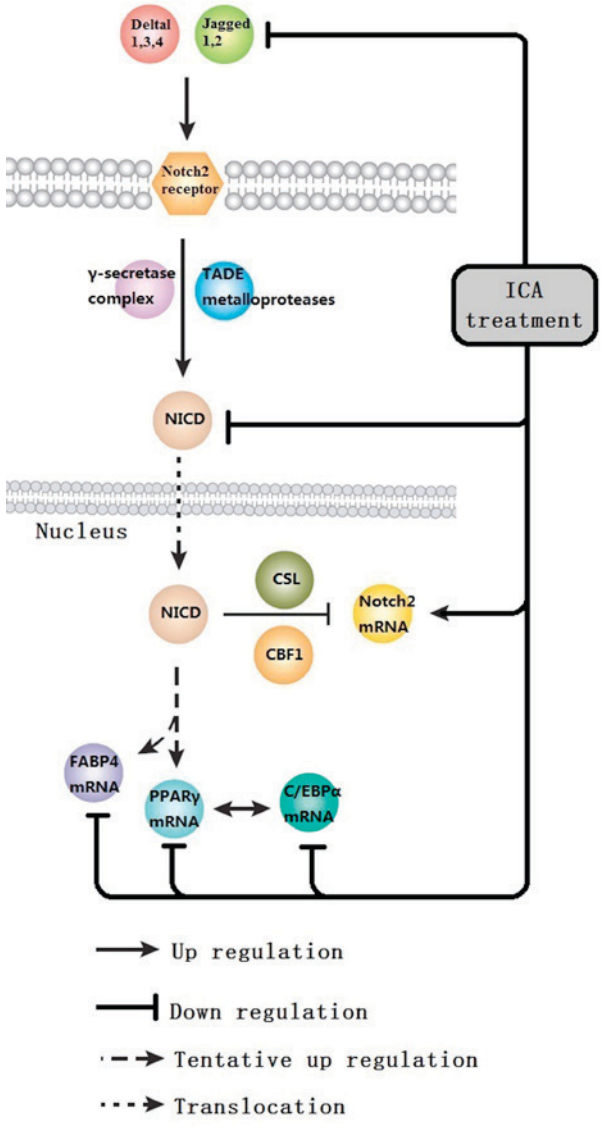

Figure 7. ICA effect diagram. ICA is likely to inhibit the differentiation of MSCs into adipocytes by suppressing the expression of PPARγ, C/EBPα and FABP4 mRNA. In addition, ICA may inhibit the production of Notch2 mRNA through the inhibition of N1ICD expression. NICD, Notch intracellular domain; FABP4, fatty acid-binding protein 4; PPARγ, peroxisome proliferator-activated receptor γ; ICA, icarrin; TADE, tetraaminodiphencyl ether; C/EBPα, CCAAT/enhancer binding protein α.

differentiation of MSCs into adipocytes and suppressed differentiation of MSCs into OB. The results of the current study suggest that ICA has a beneficial effect on OP by suppressing differentiation of MSCs into adipocytes through reduced expression of mRNA for adipogenesis correlation factors, PPARγ, C/EBPα and FABP4.

In conclusion, the current study demonstrated that ICA has a beneficial effect on OP rats, with 250 mg/kg/day being the most effective of the doses examined. With its good safety profile, ICA could be a promising candidate for further development as a way of treating and preventing OP. ICA is, however, likely to inhibit differentiation of MSCs into adipocytes by suppressing the expression of PPARγ, C/EBPα and FABP4 mRNA. ICA may also inhibit Notch2 mRNA expression through the inhibition of N1ICD expression. Further preclinical investigations will be required to better define the pharmacological targets of ICA and to dissect the associations between the different signaling pathways involved in the treatment of OP (Fig. 7).

Acknowledgements

The authors thank the International Science Editing Compuscript, Ltd. (Shannon, Ireland) for critically reading and checking the first draft. The Lunar Prodigy dual-energy X-ray absorptiometer used in this study was a generous gift from Dr Jian Gong of the Overseas Hospital and The First Affiliated Hospital of Jinan University (Guangzhong, China). The present study was supported by the National Natural Science Foundation of China (grant nos. 81173619 and 81473509) and Natural Science Foundation of Guangdong Province, China (grant no. S2012040007531).

References

1. United States Food and Drug Association, Division of Metabolism and Endocrine Drug Products: Guidelines for Preclinical and Clinical Evaluation of Agents Used in the Prevention or Treatment of Postmenopausal Osteoporosis. Food and Drug Administration, USA, 1997.
2. Cairoli E, Zhukouskaya VV, Eller-Vainicher C and Chiodini I: Perspectives on osteoporosis therapies. J Endocrinol Invest 38: 303-311, 2015.
3. An J, Yang H, Zhang Q, Liu C, Zhao J, Zhang L and Chen B: Natural products for treatment of osteoporosis: The effects and mechanisms on promoting osteoblast-mediated bone formation. Life Sci 147: 46-58, 2016.
4. Indran IR, Liang RL, Min TE and Yong EL: Preclinical studies and clinical evaluation of compounds from the genus Epimedium for osteoporosis and bone health. Pharmacol Ther 162: 188-205, 2016.
5. Sze SC, Tong Y, Ng TB, Cheng CL and Cheung HP: Herba Epimedii: Anti-oxidative properties and its medical implications. Molecules 15: 7861-7870, 2010.
6. Guo J, Li F, Wu Q, Gong Q, Lu Y and Shi J: Protective effects of icariin on brain dysfunction induced by lipopolysaccharide in rats. Phytomedicine 17: 950-955, 2010.
7. Li S, Dong P, Wang J, Zhang J, Gu J, Wu X, Wu W, Fei X, Zhang Z, Wang Y, *et al*: Icariin, a natural flavonol glycoside, induces apoptosis in human hepatoma SMMC-7721 cells via a ROS/JNK-dependent mitochondrial pathway. Cancer Lett 298: 222-230, 2010.
8. Zhou J, Wu J, Chen X, Fortenbery N, Eksioglu E, Kodumudi KN, Pk EB, Dong J, Djeu JY and Wei S: Icariin and its derivative, ICT, exert anti-inflammatory, anti-tumor effects, and modulate myeloid derived suppressive cells (MDSCs) functions. Int Immunopharmacol 11: 890-898, 2011.
9. Wang Z, Zhang X, Wang H, Qi L and Lou Y: Neuroprotective effects of icaritin against beta amyloid-induced neurotoxicity in primary cultured rat neuronal cells via estrogen-dependent pathway. Neuroscience 145: 911-922, 2007.
10. Yang L, Lu D, Guo J, Meng X, Zhang G and Wang F: Icariin from Epimedium brevicornum Maxim promotes the biosynthesis of estrogen by aromatase (CYP19). J Ethnopharmacol 145: 715-721, 2013.
11. Qin L, Han T, Zhang Q, Cao D, Nian H, Rahman K and Zheng H: Antiosteoporotic chemical constituents from Er-Xian Decoction, a traditional Chinese herbal formula. J Ethnopharmacol 118: 271-279, 2008.
12. Zhang G, Qin L, Sheng H, Yeung KW, Yeung HY, Cheung WH, Griffith J, Chan CW, Lee KM and Leung KS: Epimedium-derived phytoestrogen exert beneficial effect on preventing steroid-associated osteonecrosis in rabbits with inhibition of both thrombosis and lipid-deposition. Bone 40: 685-692, 2007.
13. Ye HY and Lou YJ: Estrogenic effects of two derivatives of icariin on human breast cancer MCF-7 cells. Phytomedicine 12: 735-741, 2005.

14. Yamaguchi M and Gao YH: Inhibitory effect of genistein on bone resorption in tissue culture. Biochem Pharmacol 55: 71-76, 1998.
15. Chen KM, Ge BF, Liu XY, Ma PH, Lu MB, Bai MH and Wang Y: Icariin inhibits the osteoclast formation induced by RANKL and macrophage-colony stimulating factor in mouse bone marrow culture. Pharmazie 62: 388-391, 2007.
16. Huang J, Yuan L, Wang X, Zhang TL and Wang K: Icaritin and its glycosides enhance osteoblastic, but suppress osteoclastic, differentiation and activity in vitro. Life Sci 81: 832-840, 2007.
17. Titorencu I, Pruna V, Jinga VV and Simionescu M: Osteoblast ontogeny and implications for bone pathology: An overview. Cell Tissue Res 355: 23-33, 2014.
18. Grogan SP, Olee T, Hiraoka K and Lotz MK: Repression of chondrogenesis through binding of notch signaling proteins HES-1 and HEY-1 to N-box domains in the COL2A1 enhancer site. Arthritis Rheum 58: 2754-2763, 2008.
19. Nobta M, Tsukazaki T, Shibata Y, Xin C, Moriishi T, Sakano S, Shindo H and Yamaguchi A: Critical regulation of bone morphogenetic protein-induced osteoblastic differentiation by Delta1/Jagged1 activated Notch1 signaling. J Biol Chem 280: 15842-15848, 2005.
20. Garcés C, Ruiz-Hidalgo MJ, Font de Mora J, Park C, Miele L, Goldstein J, Bonvini E, Porrás A and Laborda J: Notch-1 controls the expression of fatty acid-activated transcription factors and is required for adipogenesis. J Biol Chem 272: 29729-29734, 1997.
21. Akune T, Ohba S, Kamekura S, Yamaguchi M, Chung UI, Kubota N, Terauchi Y, Harada Y, Azuma Y, Nakamura K, *et al*: PPARgamma insufficiency enhances osteogenesis through osteoblast formation from bone marrow progenitors. J Clin Invest 113: 846-855, 2004.
22. Teitelbaum SL: Osteoclasts: What do they do and how do they do it? Am J Pathol 170: 427-435, 2007.
23. Devlin H and Ferguson MW: Compositional changes in rat femur following ovariectomy. Acta Anat (Baslel) 136: 38-41, 1989.
24. Kalu DN: Evaluation of the pathogenesis of skeletal changes in ovariectomized rats. Endocrinology 115: 507-512, 1984.
25. Livak KJ and Schmittgen TD: Analysis of relative gene expression data using real-tie quantitative PCR and the 2(-Delta Delta C(T)) Method. Methods 25: 402-408, 2001.
26. Mok SK, Chen WF, Lai WP, Leung PC, Wang XL, Yao XS and Wong MS: Icariin protects against bone loss induced by oestrogen deficiency and activates oestrogen receptor-dependent osteoblastic functions in UMR 106 cells. Br J Pharmacol 159: 939-949, 2010.
27. Nan H, Ma MH, Nan SS and Xu LL: Antiosteoporotic activity of icariin in ovariectomized rats. Phytomedicine 16: 320-326, 2009.
28. Feng R, Feng L, Yuan Z, Wang D, Wang F, Tan B, Han S, Li T, Li D and Han Y: Icariin protects against glucocorticoid-induced osteoporosis in vitro and prevents glucocorticoid-induced osteocyte apoptosis in vivo. Cell Biochem Biophys 67: 189-197, 2013.
29. Ma HP, Ming LG, Ge BF, Zhai YK, Song P, Xian CJ and Chen KM: Icarrin is more potent than genistein in promoting osteoblast differentiation and mineralization in vitro. J Cell Biochem 112: 916-923, 2011.
30. Zhao J, Ohba S, Shinkai M, Chung UI and Nagamune T: Icariin induces osteogenic differentiation in vitro in a BMP- and Runx2-dependent manner. Biochem Biophys Res Commun 369: 444-448, 2008.
31. Povoroznyuk Vladyslav V,; Nikonenko, Pavel I.; Grygoryeva, Natalija V. Bone 42; 1: S83-S83, 2008.
32. Peng S, Zhang G, He Y, Wang X, Leung P, Leung K and Qin L: Epimedium-derived flavonoids promote osteoblastogenesis and suppress adipogenesis in bone marrow stromal cells while exerting an anabolic effect on osteoporotic bone. Bone 45: 534-544, 2009.
33. Campa VM, Gutiérrez-Lanza R, Cerignoli F, Díaz-Trelles R, Nelson B, Tsuji T, Barcova M, Jiang W and Mercola M: Notch activates cell cycle reentry and progression in quiescent cardiomyocytes. J Cell Biol 183: 129-141, 2008.
34. Augello A and De Bari C: The regulation of differentiation in mesenchymal stem cells. Hum Gene Ther 21: 1226-1238, 2010.
35. Huang Y, Yang X, Wu Y, Jing W, Cai X, Tang W, Liu L, Liu Y, Grotkau BE and Lin Y: Gamma-secretase inhibitor induces adipogenesis of adipose-derived stem cells by regulation of Notch and PPAR-gamma. Cell Prolif 43: 147-156, 2010.
36. Bai S, Kopan R, Zou W, Hilton MJ, Ong CT, Long F, Ross FP and Teitelbaum SL: NOTCH1 regulates osteoclastogenesis directly in osteoclast precursors and indirectly via osteoblast lineage cells. J Biol Chem 283: 6509-6518, 2008.
37. Fiúza UM and Arias AM: Cell and molecular biology of Notch. J Endocrinol 194: 459-474, 2007.
38. Weinmaster G: Notch signal transduction: A real rip and more. Curr Opin Genet Dev 10: 363-369, 2000.
39. Zanotti S, Smerdel-Ramoya A, Stadmeyer L, Durant D, Radtke F and Canalis E: Notch inhibits osteoblast differentiation and causes osteopenia. Endocrinology 149: 3890-3899, 2008.
40. Ugarte F, Ryser M, Thieme S, Fierro FA, Navratiel K, Bornhäuser M and Brenner S: Notch signaling enhances osteogenic differentiation while inhibiting adipogenesis in primary human bone marrow stromal cells. Exp Hematol 37: 867-875.e1, 2009.
41. Kim HL, Sim JE, Choi HM,Choi IY, Jeong MY, Park J,Jung Y, Youn DH, Cho JH,Kim JH, *et al*: The AMPK pathway mediates an anti-adipogenic effect of fruits of Hovenia dulcis Thunb. Food Funct 5: 2961-2968, 2014.
42. Lewis J, Hanisch A and Holder M: Notch signaling, the segmentation clock, and the patterning of vertebrate somites. J Biol 8: 44, 2009.